Susceptibility and magnetization of $CuMn(S_2C_2O_2)_2 \cdot 7.5H_2O$. First experimental and theoretical characterization of a quasi-one-dimensional ferrimagnetic chain

M. Verdaguer
Laboratoire de Spectrochimie des éléments de transition (Equipe de Recherche No. 672 associée au Centre National de la Recherche Scientifique), Université de Paris—Sud, F-91405 Orsay, France

A. Gleizes
Laboratoire de Chimie de Coordination du Centre National de la Recherche Scientifique, 205 route de Narbonne, F-31400 Toulouse, France

J. P. Renard and J. Seiden
Institut d'Electronique Fondamentale (Laboratoire associé au Centre National de la Recherche Scientifique), Université de Paris—Sud, F-91405 Orsay, France
(Received 23 September 1983)

The quasi-one-dimensional compound $CuMn(S_2C_2O_2)_2 \cdot 7.5H_2O$ was synthesized, and its magnetic susceptibility χ_M was measured in the temperature range $T=4.2$—240 K. The curve $\chi_M T$ vs T presents a minimum at 130 K and a maximum at $\simeq 7.5$ K where three-dimensional ordering occurs. Magnetization data at 1.3 and 4.2 K in the field range 0—5 T are consistent with an antiferromagnetic interaction between Cu(II) and Mn(II) through the dithioxalato bridge. We present theoretical calculations for isotropic exchange interactions between quantum spins $\frac{1}{2}$ (Cu^{2+}) and classical spins (Mn^{2+}). The susceptibility is calculated numerically. This theoretical model fits the experimental data well, allowing the determination of the coupling constant J as -30.3 cm^{-1}. The antiferromagnetic interaction between Cu(II) and Mn(II) metallic ions leads to a *one-dimensional ferrimagnetic behavior,* characterized for the first time, both experimentally and theoretically.

I. INTRODUCTION

Experimental and theoretical studies devoted to one-dimensional (1D) magnetic systems remain a very active area of solid-state-physics research.[1-3] Quasi-1D materials with various spin numbers, with both ferromagnetic (F) or antiferromagnetic (AF) interactions have been synthesized and studied. $(CH_3)_4NMnCl_3$ (TMMC) is one of the best examples of a 1D Heisenberg antiferromagnet with $S=\frac{5}{2}$,[4] whereas $(CH_3)_4NCuCl_3$ (TMCuC) is a good model for an $S=\frac{1}{2}$ linear ferromagnet.[5,6]

Alternating chains of identical spins with different coupling constants J_1 and J_2 are known and theoretically studied,[7-9] as well as doped materials of S_A spins in a 1D system of S_B spins, with the same coupling constant J between the spins. C. Dupas *et al.* reported recently on a quasi-1D chain $(CH_3)_4NMn_xCu_{1-x}Cl_3$ with x ranging from 0 to 1.[10] Until recently, however, no bimetallic chain of structurally ordered alternating spins S_A and S_B with a uniform J value along the chain, was reported.

In the present work, we studied the first bimetallic chain with two different paramagnetic ions, Cu^{2+} and Mn^{2+}, structurally ordered in an alternating manner: $CuMn(S_2C_2O_2)_2 \cdot 7.5\ H_2O$ (CuMnDTO). The two ions are bridged by a polyatomic bischelating ligand, the dithioxalato anion $S_2C_2O_2^{2-}$. The crystallographic structure which has been fully refined is presented in Sec. II.[11,12] We measured the susceptibility at low field, and the magnetization of the compound in the field range 0.5 T (Secs. II and III).

To the best of our knowledge, no calculation has been done on a system of alternating spins $\frac{1}{2}$ and $\frac{5}{2}$. Only one paper has appeared on Heisenberg chains with alternating quantum and classical spins.[13] We present in Sec. IV a theoretical model for the magnetic susceptibility in the whole temperature range, for an alternating system of quantum spins $\frac{1}{2}$ (Cu^{2+}) and classical spins (Mn^{2+}). The problem is solved numerically by the diagonalization of a 6th order symmetric matrix. This numerical method allows us to find the expected minimum in the $\chi_M T$ vs T curve[14] and to give a value for the intrachain coupling constant J. We used an isostructural analog of CuMnDTO, $PdMn(S_2C_2O_2)_2 \cdot 7.5\ H_2O$, to determine the interchain coupling constant J'.

II. EXPERIMENTAL TECHNIQUES

A. Synthesis and crystal structure

We synthesized CuMnDTO by mixing concentrated aqueous solutions of $K_2Cu(S_2C_2O_2)_2$ and $MnSO_4 \cdot H_2O$ and slowly cooling down. Small brown monocrystals are obtained. They are suitable for x-ray analysis: The crystal structure has been reported elsewhere.[11,12] The space group is monoclinic $P2_1/c$ (C_{2h}^5) with four formula units in cells of dimensions $a=11.692(2)$ Å, $b=20.665(5)$ Å, $c=7.360$ Å, and $\beta=[103.84(2)]°$. The structure is sketched in Figs. 1 and 2: It consists of chains $\cdots Cu(S_2C_2O_2)Mn(H_2O)_3(O_2C_2S_2)\cdots$, criss-crossing glide planes c and stacking along these planes. Each layer

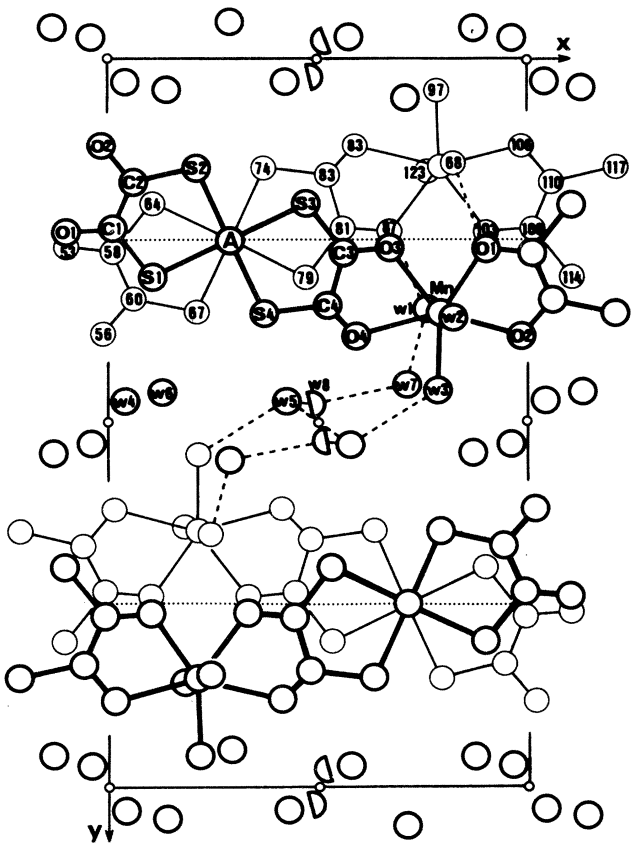

FIG. 1. Ball and spoke drawing of the structure of $AMn(S_2C_2O_2)_2 \cdot 7.5\ H_2O$ (A = Cu, Pd) in projection onto the (001) plane. Glide planes c and centers of inversion are represented with conventional crystallographic symbols.

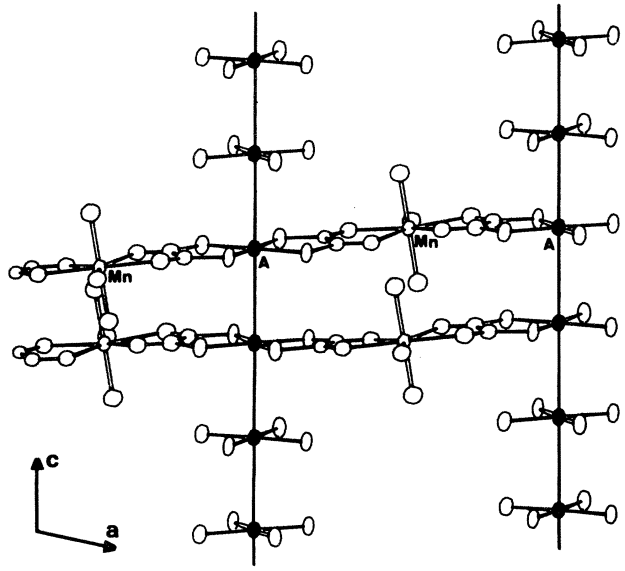

FIG. 2. A partial view down the b axis of a layer of stacked $\cdots A(S_2C_2O_2)Mn(H_2O)_3(O_2C_2S_2)\cdots$ chains, emphasizing the columnar structure generated by the AS_4 fragments. A atoms (Cu in CuMnDTO and Pd in PdMnDTO) are shown as black ellipsoids.

of stacked chains is separated from the next one by intervening water molecules. Figure 1 shows how two chains are related within a layer. Copper(II) is in a sulfur square-planar environment, manganese(II) is heptacoordinated in a pentagonal bipyramidal surrounding. The copper-manganese distance is about 6 Å. Figure 2 exhibits the stacking distance between two copper ions belonging to neighboring chains: $d_{Cu\text{-}Cu} = 3.681$ Å, which is the nearest distance between two chains in the stack; $d_{Mn\text{-}Mn} = 5.6$ Å. The crystals are air stable but sensitive to loss of water: A dehydrated black variety exists, containing three water molecules with quite different magnetic properties.[12]

We synthesized $PdMn(S_2C_2O_2)_2 \cdot 7.5\ H_2O$ (PdMnDTO) in a manner similar to that used for CuMnDTO, using $K_2Pd(S_2C_2O_2)_2$ instead of $K_2Cu(S_2C_2O_2)_2$. The crystals obtained are ribbon-shaped, orange, and the compound is isostructural with CuMnDTO.[12] ($a = 11.79$ Å, $b = 20.78$ Å, $c = 7.31$ Å, $\beta = 103.5°$)

B. Susceptibility measurements

The magnetic susceptibility was measured in the range 4.2–240 K using a Faraday-type magnetometer equipped with a continuous-flow cryostat designed by Oxford Instruments. The temperature is given by a gold-iron/chromel thermocouple. A magnetic field of 0.12 T was used. Independence of the susceptibility on the magnetic field was checked at 240 K. Mercury tetrakis (thiocyanato) cobaltate (II) was used as a susceptibility standard. The absolute accuracy in temperature was estimated at ± 0.1 K and the relative accuracy on the apparent increase of the weight of the sample with applied field at about 1%. The correction of diamagnetism was estimated at 226.5 10^{-6} $cm^3\,mol^{-1}$ for CuMnDTO. The compound can lose water molecules by degassing at room temperature. Thus we begin the experiment at 240 K, pumping the sample compartment at this temperature.

C. Magnetization measurements

The magnetization of CuMnDTO has been measured as a function of the magnetic field H, at 1.3 and 4.2 K by means of a fluxmetric method. The sample was extracted from a pickup coil of about 40 000 turns of thin copper wires immersed in the helium bath. The induced voltage was integrated and displayed on a XT recorder. The fluxmeter was calibrated from the well known magnetization of a chromium-potassium-alum sphere. The field was supplied by a 6 T superconducting magnet calibrated by Al nuclear magnetic resonance for $H > 0.1$ T, and by a nitrogen-cooled copper solenoid for $H < 0.15$ T. The cryogenic apparatus has been described in detail in a previous paper.[15]

III. EXPERIMENTAL RESULTS

A. Susceptibility

The temperature dependence of the molar susceptibility χ_M, shown in Fig. 3 as the product $\chi_M T$ vs T, exhibits three main features: (i) the existence of a minimum of

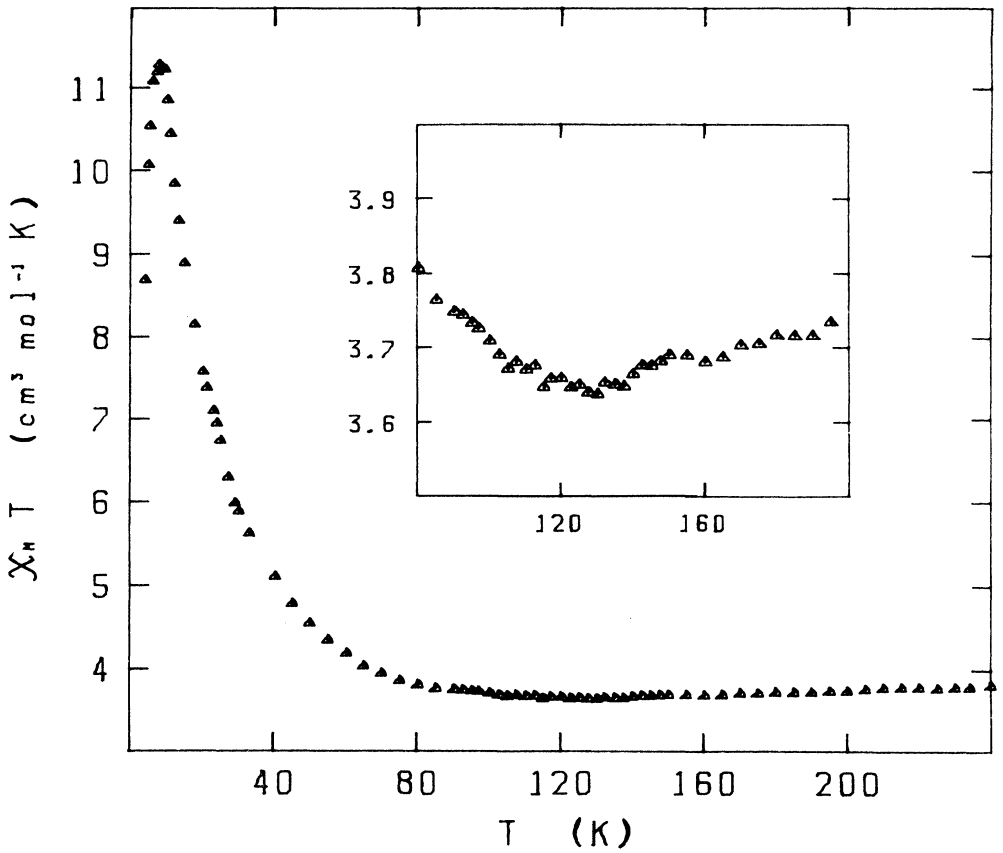

FIG. 3. Experimental temperature dependence of the molar susceptibility of CuMnDTO as $\chi_M T$ vs T. The molecular weight is the one of the fragment $CuMn(S_2C_2O_2)_2 \cdot 7.5\ H_2O$.

$\chi_M T$ at 130 K, when $\chi_M T = 3.64\ cm^3 mol^{-1} K$, (ii) a sharp increase between 130 and 7.5 K, and (iii) after a maximum at 7.5 K, a decrease of $\chi_M T$ down to 4.2 K.

The susceptibility behavior in (i) and (ii) is consistent with the one of an alternating chain of copper (II) ions, spin $\frac{1}{2}$, and manganese (II) ions, spin $\frac{5}{2}$, antiferromagnetically coupled through the dithioxalato anion: At high temperature, $\chi_M T$ tends towards the paramagnetic limit; the minimum corresponds to a short-range order state where the copper spins are antiparallel to the manganese ones, without significant correlation between neighboring manganese ions; when temperature decreases, the correlation length in the chain increases, leading to a *ferrimagnetic short-range order.*

The decrease between 7.5 and 4.2 K may be assigned to a three-dimensional ordering (3D), as a consequence of antiferromagnetic coupling between the chains.

Such antiferromagnetic interchain coupling can be evaluated with the nickel(II) or the palladium(II) compounds $AMn(S_2C_2O_2)_2 \cdot 7.5\ H_2O$ [A=Ni(II), Pd(II), diamagnetic ions], isostructural of the copper derivative.

The temperature dependence of the molar susceptibility of the palladium-manganese chain PdMnDTO is given in Fig. 4 as χ_M^{-1} vs T, in the temperature range 4.2—40 K. The experimental data are consistent with a Curie-Weiss behavior of manganese(II) ions,

$$\chi_M = \frac{C}{T-\Theta}\ , \tag{1}$$

where the Curie constant $C = 4.39\ mol\,cm^3\,K$ and the Curie-Weiss temperature $\Theta = -1.8$ K. Applying the mean-field approximation to a 1D system of manganese(II) ions, with two nearest neighbors, and a J' interaction between two neighboring manganese, we can write

$$\Theta = \frac{4}{3}\frac{J'}{\kappa} S(S+1)\ , \tag{2}$$

where κ is the Boltzmann constant and $S = \frac{5}{2}$. A J' value can be deduced: $J' = -0.16$ K ($-0.11\ cm^{-1}$). The coupling can occur either between manganese(II) ions belonging to the same chain, or between manganese ions from neighboring chains (J' interchain). The second hypothesis is the most likely: The intrachain manganese-manganese distance is about 12 Å, where as the closest interchain manganese-manganese length is about 5.6 Å, with a hydrogen-bond pathway $Mn \cdots OH_2 \cdots H_2O \cdots Mn$ seen in Fig. 1.

The intrachain interaction between copper(II) and manganese(II) ions will be estimated in Sec. V, after the theoretical treatment of Sec. IV.

B. Magnetization

The experimental data reported in Fig. 5, show three different features.

(i) A fast initial increase of M(H) for $H < 3.10^{-2}$T, indicating a large value of the susceptibility when $H \to 0$.

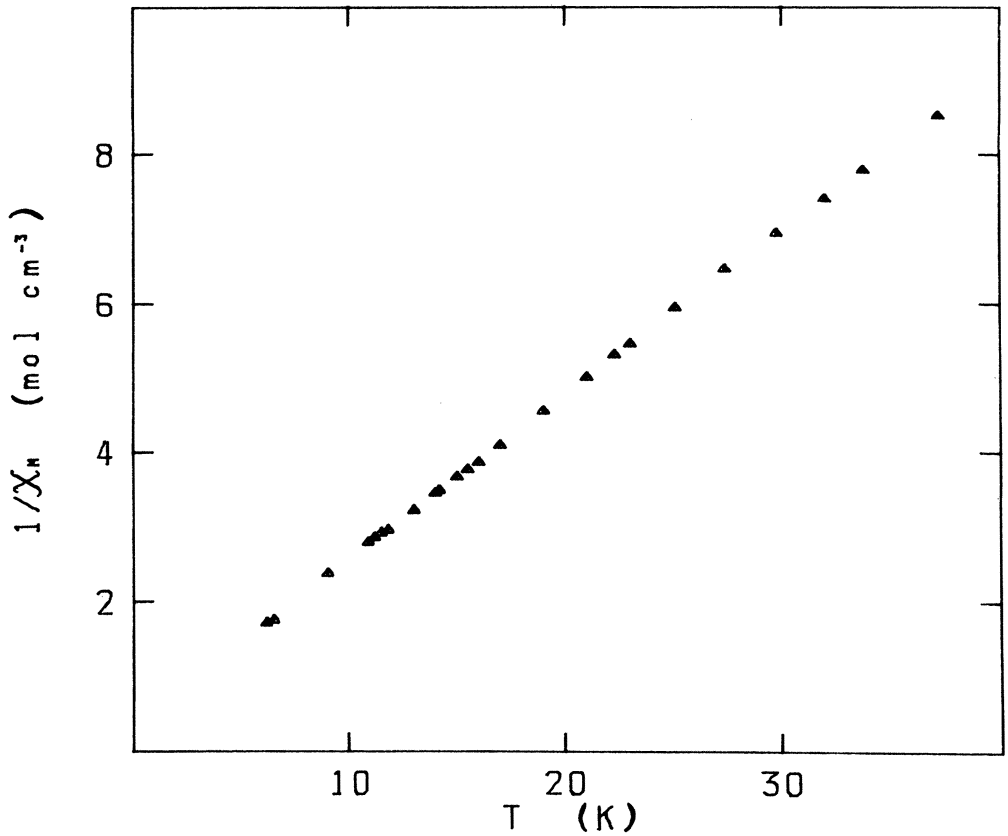

FIG. 4. Experimental temperature dependence of the molar susceptibility of PdMnDTO as χ_M^{-1} vs T. The molecular weight is the one of the fragment PdMn $(S_2C_2O_2)_2 \cdot 7.5H_2O$.

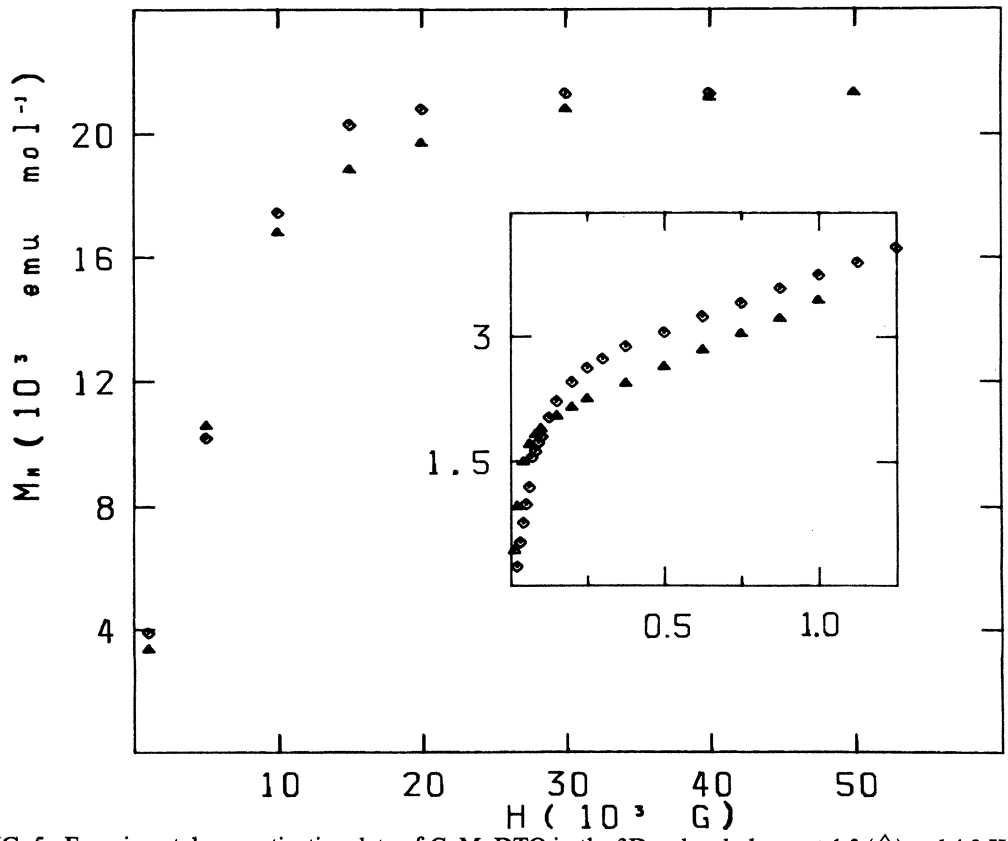

FIG. 5. Experimental magnetization data of CuMnDTO in the 3D ordered phase, at 1.3 (◇) and 4.2 K (△).

(ii) In the field range 3×10^{-2}—1 T, a linear increase of M(H) with a smaller slope.

(iii) A well-defined saturation of $M(H)$ at higher field values. The saturation magnetization M_S at $H=5$ T is in good agreement with

$$M_S=g\mu_B(S-s)\ , \tag{3}$$

where $g\simeq1.9$, μ_B is the Bohr magneton, and S and s are the manganese and copper spins, respectively. It is consistent with the hypothesis of weakly coupled ferrimagnetic chains with opposite directions of the copper and manganese spins. The linear increase of $M(H)$ below the saturation field $H_S\sim1.2$ T is related to the progressive aligment of the antiferromagnetically coupled ferrimagnetic chains along the field. In the molecular-field approximation,

$$H_S=\frac{4z'\,|\,J'\,|\,S}{g\mu_B}\ , \tag{4}$$

where z' is the number of neighboring chains and J' the interchain exchange. Using $g=2$ and $z'=2$, one obtains from the experimental H_S value, $J'/\kappa\simeq-0.1$ K, in satisfactory agreement with the value deduced from the PdMnDTO susceptibility (−0.16 K).

The fast increase of the initial magnetization is likely due to a canting of the ferrimagnetic moments of the chains giving rise to weak ferromagnetism (WF). The WF moment is determined from the intersect of the linear part of $M(H)$ with $H=0$ axis. The tilt angle θ is given by

$$\sin\theta=M_{\rm WF}/M_S\ . \tag{5}$$

Its experimental value is $\theta=6.35$. The WF behavior of CuMnDTO at low temperature has been also observed by ac susceptibility measurements between 1.3 and 4.2 K. The ac susceptibility is very large at 4.2 K and decreases with decreasing temperature. On the other hand, the WF behavior has not been observed in the Faraday balance-magnetization measurements in which the sample is slowly cooled down to 4.2 K. The low-temperature magnetic phase of CuMnDTO might depend on the sample cooling rate. A similar phenomenon was recently observed on the 1D system $N(C_2H_5)_4FeCl_4$.[16] Further investigations are clearly needed to clear up this point.

IV. THEORY

A. Hamiltonian

X-ray structure shows that copper(II) and manganese(II) ions align in structurally ordered alternating chains —Cu—Mn—Cu—Mn—$\cdots$; magnetic data shows that the chains are well insulated magnetically from each other. Considering that all anisotropic interactions, including the dipolar couplings, are small, we take as Hamiltonian for the alternating chain:

$$\mathcal{H}=-J\sum_{i=1}^{N}(\vec{\mathrm{S}}_i+\vec{\mathrm{S}}_{i+1})\cdot\vec{\mathrm{s}}_i-g\mu_BH\left[\sum_{i=1}^{N+1}S_{zi}+\sum_{i=1}^{N}s_{zi}\right]\ . \tag{6}$$

$\vec{\mathrm{s}}_i$, the spin of the copper(II) ions, is a quantum spin $s=\frac{1}{2}$; $\vec{\mathrm{S}}_i$, the spin of the manganese(II) ions, is a classical spin and is considered as a classical vector; H is the magnetic field, parallel to the z axis; J is the intrachain coupling constant between s and S spins.

It is possible to solve the Hamiltonian in Eq. (6), with $H=0$, and to obtain a closed form for the zero-field susceptibility: For that, we have derived analytically spin correlations between quantum spins, between classical spins and between quantum spins and classical ones.[17]

We prefer to present here another theoretical method, which is only valid to order S^{-1}, but which, we believe partially takes into account the quantum character of the $S=\frac{5}{2}$ spins. We write

$$\mathcal{H}=\sum_{i=1}^{N}\mathcal{H}_i\ ,$$

$$\mathcal{H}_i=-J\vec{\mathcal{S}}_i\cdot\vec{\mathrm{s}}_i-g\mu_BH\left[\frac{\mathcal{S}_{zi}}{2}+s_{zi}\right]\ , \tag{7}$$

$$\vec{\mathcal{S}}_i=\vec{\mathrm{S}}_i+\vec{\mathrm{S}}_{i+1}\ .$$

$\mathcal{H}_i$ is an operator, depending upon $\vec{\mathrm{s}}_i$; its two eigenvalues are

$$\tfrac{1}{2}[\pm(J^2\mathcal{S}^2+g^2\mu_B^2H^2+2g\mu_BHJ\mathcal{S}_z)^{1/2}-g\mu_BH\mathcal{S}_z]\ . \tag{8}$$

We are interested in the partition function Z and the free energy F of the system:

$$Z=\mathrm{Tr}\exp\left[-\beta\sum_i\mathcal{H}_i\right]\ ,$$

$$F=-\frac{1}{\beta}\ln Z\ , \tag{9}$$

where $\beta=1/kT$ and the trace is calculated by summing over all the eigenstates of $\mathcal{H}_i$ and integrating over all the vectors $\vec{\mathrm{S}}_i$. As $\vec{\mathrm{S}}_i$ are classical vectors, all the operators $\mathcal{H}_i$ commute, and

$$Z=\mathrm{Tr}\prod_i\exp(-\beta\mathcal{H}_i)\ . \tag{10}$$

We calculate, first, the trace over the $\vec{\mathrm{s}}_i$, and using (8) we find

$$\mathrm{Tr}_{(s_i)}\exp(-\beta\mathcal{H}_i)=2\exp\left[\frac{\beta}{2}g\mu_BH\mathcal{S}_{zi}\right]\cosh[\tfrac{1}{2}\beta(J^2\mathcal{S}_i^2+2g\mu_BJH\mathcal{S}_{zi}+g^2\mu_B^2H^2)^{1/2}]\equiv P(i,i+1)\ , \tag{11}$$

and we have

$$Z=\mathrm{Tr}_{(S_i)}\prod_{i=1}^{N}P(i,i+1)\ , \tag{12}$$

where the trace means integration over all the $\vec{S}_i$. This integration is very difficult to perform and we find easier to consider in (12) all the S_i as quantum operators and to calculate the trace over the $(2S+1)^{N+1}$ eigenstates in the S_i space. As eigenstates, we choose all the eigenstates $|m_i\rangle$ of the S_{zi}, whence

$$Z=\sum_{\{m_i\}}\langle m_1,\ldots,m_i,\ldots,m_{N+1}|P(1,2)\cdots P(i,i+1)\cdots P(N,N+1)|m_1,\ldots,m_i,\ldots,m_{N+1}\rangle . \tag{13}$$

Our calculation of the static properties will then be exact to order S^{-1}, if we succeed in evaluating (13).

B. Partition function

Each of the $P(i,i+1)$ depends only on two neighboring spins $\vec{S}_i$ and $\vec{S}_{i+1}$ and we may rewrite Eq. (13) as

$$Z=\sum_{\{m\}}\cdots\times\langle m_{i-1},m_i|P(i-1,i)|m'_{i-1}m'_i\rangle\langle m'_i,m'_{i+1}|P(i,i+1)|m_i,m_{i+1}\rangle\times\cdots . \tag{14}$$

Unfortunately, nondiagonal matrix elements of the P operators appear in (14) because these P are not diagonal in the $\{m\}$ representation chosen to evaluate the trace. But, as $P(i,i+1)$ depends only on $S_{zi}+S_{z,i+1}$ and $|\vec{S}_i+\vec{S}_{i+1}|$, matrix elements of $P(i,i+1)$ are nonvanishing only if

$$m'_i+m'_{i+1}=m_i+m_{i+1} . \tag{15}$$

We define a new matrix $\underline{M}$ by

$$\langle m_{i-1},m'_{i-1}|M|m'_i,m_i\rangle=\langle m_{i-1},m_i|P(i-1,i)|m'_{i-1},m'_i\rangle , \tag{16}$$

and using (14), we find

$$Z=\mathrm{Tr}(\underline{M}^N) . \tag{17}$$

The matrix $\underline{M}$ plays the role of a transfer matrix; it is symmetrical in the permutation of row and column indices and therefore, its eigenvalues are real.

If $N\to\infty$ and if $\underline{M}$ has a greatest eigenvalue Λ, we have

$$Z\simeq\Lambda^N,\quad F=-\frac{1}{\beta}N\ln\Lambda . \tag{18}$$

C. Matrix elements

By Eq. (15) we have

$$\Delta_{i-1}=m_{i-1}-m'_{i-1}=m'_i-m_i\equiv\Delta_i . \tag{19}$$

[Note the order of the eigenstate indices m_{i-1}, m'_{i-1}; m'_i, m_i in the definition (16) of the matrix elements of M and (19) of the Δ functions.] The possible values of Δ are $2S$, $2S-1,\ldots,1,0,-1,\ldots,-2S$. In order to write out the matrix $\underline{M}$ explicitly, we first write all matrix elements with $\Delta=2S$, then those with $\Delta=2S-1$, and so on, until $\Delta=-2S$. In this way, the matrix $\underline{M}$ may be reduced to the following diagonal form:

$$\underline{M}=\begin{bmatrix}\underline{M}_{2S} & & & & & & \\ & \underline{M}_{2S-1} & & & & & \\ & & \ddots & & & & \\ & & & \underline{M}_0 & & & \\ & & & & \ddots & & \\ & & & & & \underline{M}_{-2S+1} & \\ & & & & & & \underline{M}_{-2S}\end{bmatrix} , \tag{20}$$

where the diagonal elements are matrices. $\underline{M}_K$ is the matrix containing all the matrix elements of $\underline{M}$ with $\Delta=K$. The order of the matrix $\underline{M}_K$ is $2S+1-|K|$. The matrix $\underline{M}_0$, of order $2S+1$, has $\Delta=0$ and so it contains only the diagonal matrix elements of the matrices $P(i-1,i)$. The operators $P(i-1,i)$ defined by (11) are diagonal in the representation $|\mathcal{S},\mathcal{S}_z\rangle$. So, in order to calculate the matrix elements of $\underline{M}$, we may write

$$\langle m'_i,m_i|M|m_{i+1},m'_{i+1}\rangle=\sum_{\mathcal{S}_i}\langle m'_i,m'_{i+1}|\mathcal{S}_i,\mathcal{S}_{zi}\rangle\langle\mathcal{S}_i,\mathcal{S}_{zi}|P(i,i+1)|\mathcal{S}_i,\mathcal{S}_{zi}\rangle\langle\mathcal{S}_i,\mathcal{S}_{zi}|m_i,m_{i+1}\rangle , \tag{21}$$

$$\langle\mathcal{S}_i,\mathcal{S}_{zi}|P(i,i+1)|\mathcal{S}_i,\mathcal{S}_{zi}\rangle=2\exp\left[\frac{\beta}{2}g\mu_BH\mathcal{S}_{zi}\right]\cosh\left[\frac{\beta}{2}(J^2\mathcal{S}_i^2+2g\mu_BJH\mathcal{S}_{zi}+g^2\mu_B^2H^2)^{1/2}\right] . \tag{22}$$

The sum over $\mathcal{S}_i$ in (21) runs from $\mathcal{S}_i=|\mathcal{S}_{zi}|$ to $\mathcal{S}_i=2S$. The $\langle m'_i,m'_{i+1}|\mathcal{S}_i,\mathcal{S}_{zi}\rangle$ are the Clebsch-Gordan coefficients which allow the transformation from the $|m'_i,m'_{i+1}\rangle$ to the $|\mathcal{S}_i,\mathcal{S}_{zi}\rangle$ eigenstates. One has $\mathcal{S}_{zi}=S_{zi}+S_{zi+1}=m'_i+m'_{i+1}$.

D. Expansion of eigenvalues as power series in H

We now show that the expansion in powers of H of the $2S+1$ eigenvalues of the matrix $\underline{M}_0$ contains only even powers of H. The importance of this fact will appear

below. We put

$$\langle m_{i-1},m_{i-1}\,|\,M\,|\,m_i',m_i'\rangle=(\underline{M}_0)_{m,m'}\ . \tag{23}$$

We may first write the rows m and the columns $\underline{m}'$ in the order $S, S-1\ldots,-S$. ($S=\frac{5}{2}$.) But we may also write the rows m and the columns m' in the reverse order $-S,-(S-1),\ldots,S$. In this second formulation, the place of $(\underline{M}_0)_{m,m'}$ is taken up by $(\underline{M}_0)_{-m,-m'}$; so, the eigenvalues λ_0 of $\underline{M}_0$, which are functions $f(\ldots,(\underline{M}_0)_{m,m'},\ldots)$ of all the matrix elements $(\underline{M}_0)_{m,m'},\ldots$ are the *same* functions of $(\underline{M}_0)_{-m,-m'}$,

$$\begin{aligned}\lambda_0&=f(\ldots,(\underline{M}_0)_{m,m'},\ldots,)\\&=f(\ldots,(\underline{M}_0)_{-m,-m'},\ldots)\ .\end{aligned} \tag{24}$$

Suppose first that $H=0$. By

$$\langle m,m'\,|\,\mathscr{S},\mathscr{S}_z\rangle=(-1)^{\mathscr{S}_z}(2\mathscr{S}+1)^{1/2}\begin{pmatrix}S & S & \mathscr{S}\\ m & m' & -\mathscr{S}_z\end{pmatrix},$$
$$\begin{pmatrix}S & S & \mathscr{S}\\ -m & -m' & \mathscr{S}_z\end{pmatrix}=-(-1)^{2S+\mathscr{S}}\begin{pmatrix}S & S & \mathscr{S}\\ m & m' & -\mathscr{S}_z\end{pmatrix}, \tag{25}$$

which gives the Clebsch-Gordan coefficients in terms of Wigner's $3j$ symbols, we have, using Eqs. (21) and (22), $(M_0)_{m,m'}=(M_0)_{-m,-m'}$. Now, switch on H. In the substitution $m,m'\to-m,-m'$, we have $\mathscr{S}_z\to-\mathscr{S}_z$. Because the odd powers of H in Eq. (17) are multiplied by $\mathscr{S}_z$, in the presence of H, we have

$$[M_0(H)]_{m,m'}=[M_0(-H)]_{-m,-m'}\ , \tag{26}$$

and by (24)

$$\lambda_0(H)=\lambda_0(0)+b_0H^2+\cdots\ . \tag{27}$$

We observe that (27) is not verified by the eigenvalues of the other $\underline{M}_K$ ($K\neq0$) appearing in (20). However, following the same lines, we can associate to each eigenvalue λ_K of $\underline{M}_K$, an eigenvalue λ_{-K} of $\underline{M}_{-K}$ such as

$$\begin{aligned}\lambda_K(H)&=\lambda_K(0)+a_KH+b_KH^2+\cdots\ ,\\ \lambda_{-K}(H)&=\lambda_K(0)-a_KH+b_KH^2+\cdots\ .\end{aligned} \tag{28}$$

E. Greatest eigenvalue

We show now that the greatest eigenvalue of the matrix $\underline{M}$ is one of the eigenvalues of $\underline{M}_0$ at high temperatures, such that $\beta\,|\,J\,|\,S\ll1$. We expand (22) as a power series in $\beta\,|\,J\,|\,S$,

$$\langle\mathscr{S},\mathscr{S}_z\,|\,P\,|\,\mathscr{S},\mathscr{S}_z\rangle=2\exp\left[\frac{\beta}{2}g\mu_BH\mathscr{S}_z\right]\left[1+\sum_{n=1}^{\infty}\frac{1}{(2n)!}\left[\frac{\beta}{2}\right]^{2n}(J^2\mathscr{S}^2+2g\mu_BJH\mathscr{S}_z+g^2\mu_B^2H^2)^n\right]\ . \tag{29}$$

But

$$\sum_i\langle m_{i-1},m_i\,|\,\mathscr{S}_i,\mathscr{S}_{zi}\rangle\langle\mathscr{S}_i,\mathscr{S}_{zi}\,|\,m_{i-1}'m_i'\rangle=\delta_{m_{i-1},m_{i-1}'}\delta_{m_i,m_i'}\ . \tag{30}$$

If the field H is vanishingly small, by (21) all matrix elements of $\underline{M}_K$ with $K\neq0$ are of the order of $(\beta JS)^2$. It follows for the eigenvalues $\lambda_K(0)$, $K\neq0$ that

$$\lambda_K(0)\propto(\beta JS)^2,\quad\beta\,|\,J\,|\,S\ll1\ . \tag{31}$$

But it may be shown that when $H=0$, the greatest eigenvalue Λ of $\underline{M}$ is given by

$$\Lambda(0)\simeq4(2S+1)\left[\frac{\sinh(\beta JS)}{\beta JS}-\frac{\cosh(\beta JS)}{(\beta JS)^2}+\frac{1}{(\beta JS)^2}\right], \tag{32}$$

which, if $\beta\,|\,J\,|\,S\ll1$, reduces to

$$\Lambda(0)\simeq(2S+1)[2+\tfrac{1}{2}(\beta JS)^2]\ . \tag{33}$$

So, if $\beta\,|\,J\,|\,S\ll1$, $\Lambda(0)$ cannot be an eigenvalue of $\underline{M}_K$ with $K\neq0$. We may suppose that this property can be extended to low temperatures: If it is not verified, there must exist a temperature T_c, where $\lambda_K^g(0)$, the greatest eigenvalue of some matrix $\underline{M}_K$, crosses the high-temperature greatest eigenvalue $\Lambda(0)$ of $\underline{M}_0$ and we would find a phase transition at T_c: This is known to be impossible in a 1D system.[18]

F. Susceptibility

The susceptibility of the chain, using Eq. (18), is given by

$$\chi=\frac{\partial^2F}{\partial H^2}=\frac{N}{\beta}\frac{\partial^2\ln\Lambda(H)}{\partial H^2}\ , \tag{34}$$

where $\Lambda(H)$ is the greatest eigenvalue $\Lambda_0^g(H)$ of $\underline{M}_S$, i.e., the greatest eigenvalue of $\underline{M}_0$. We have computed the matrix elements of $\underline{M}_0$, using (22) and we have checked, at different values of $kT/|J|$ that the relation (27) holds for small values of $g\mu_BH/kT$. We have checked, too, that at all temperatures of interest, Eq. (32) is verified.

This allowed us to compute the susceptibility at different $kT/|J|$, using relation (34), and the values of Λ at $g\mu_BH/kT=0$ and 10^{-2}.[19] The numerical results are given in Fig. 6 as a plot of $\chi_MT(4/Ng^2)$ vs $kT/|J|$. The reduced χ_MT value tends towards the paramagnetic limit (4.75 $\mathrm{cm^3\,mol^{-1}\,K}$) at high $kT/|J|$, presents a minimum (4.035 $\mathrm{cm^3\,mol^{-1}}$ K) at $kT\,|\,J|=2.98$ and diverges at low $kT/|J|$.

Also shown in Fig. 6 are two curves obtained in the case of quantum rings of N Cu-Mn pairs, with $N=3$ (curve 2) and $N=2$ (curve 3). The method used is fully described

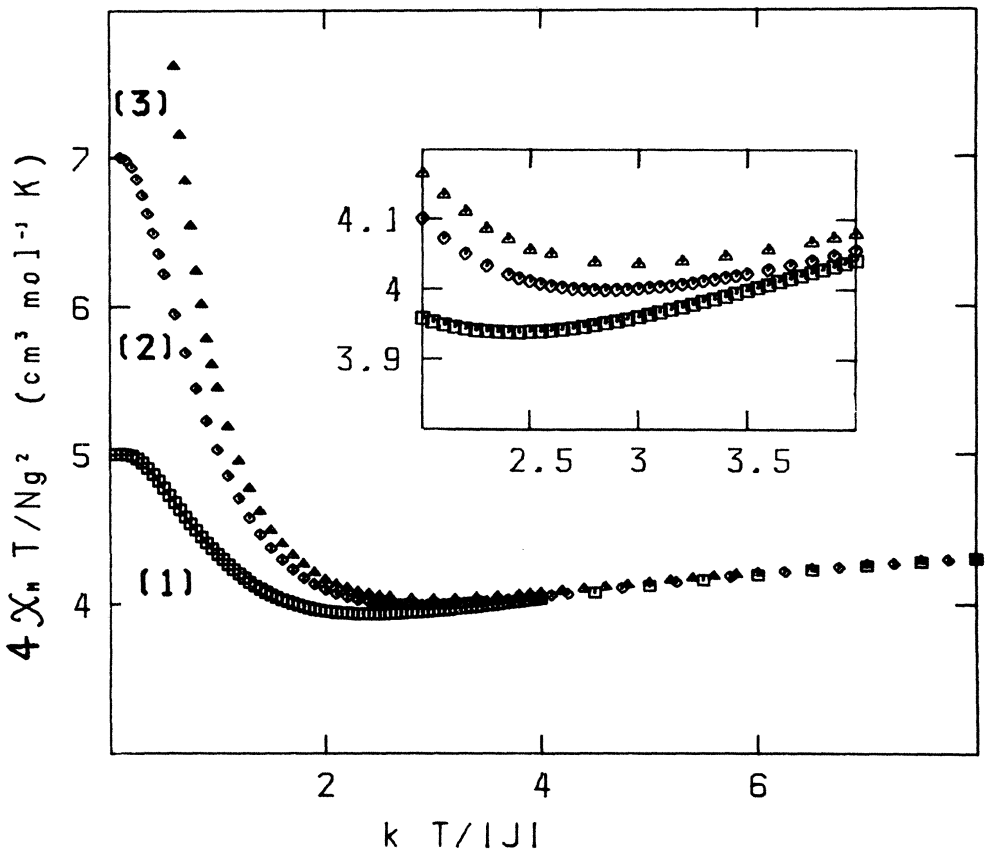

FIG. 6. Theoretical dependence of $\chi_M T$ $(4/Ng^2)$ vs $kT/|J|$ for curve 1: a ring of two pairs of alternating quantum spins $\frac{1}{2}$ and $\frac{5}{2}$ (□); curve 2: a ring of three pairs of alternating quantum spins $\frac{1}{2}$ and $\frac{5}{2}$ (◇); curve 3: a chain of $\frac{1}{2}$ quantum spins and alternating classical ones (△).

elsewhere (Refs. 8, 12, 14, 20, and 21). It consists in an exact calculation in zero field of the eigenvalues and corresponding total spins of all the eigenstates of the quantum system, from which thermodynamical properties are derived. Extrapolation to the thermodynamic limit $(N \rightarrow \infty)$ was difficult owing to the handling of a 2246th order matrix in the case where $N=4$, only. Nevertheless, it is possible to expect a rapid convergence of the curves as $N \rightarrow \infty$ (Refs. 14 and 22) and a $kT/|J|$ value at the minimum not far from 3. (As we could not reach quantitatively the thermodynamic limit, we undertook the quantum-classical calculation above.) The main point is that both approaches reproduce the behavior expected for $\chi_M T$ of an alternating chain, with a fair agreement between the two approaches. Comparison with experiment is discussed in the next section.

V. DISCUSSION

We purpose to discuss the three following points: the value of the intrachain interaction, the one-dimensional character of CuMnDTO, and the divergence of χ_m at low temperature.

A. Determination of J intrachain interaction

The J coupling intrachain constant between copper and manganese ions, through the dithioxalato bridge, and the mean g factor for the copper-manganese pair, can be deduced from the values at the minimum of the experimental and theoretical curves giving $\chi_M T$, by setting them on the same scale. It becomes $J=-43.6$ K (30.3 cm^{-1}) and $g=1.90$. The fit between experimental and theoretical results, using these values, is shown in Fig. 7. Agreement between the two curves is surprisingly good. On one hand the minimum shape is flat and a great uncertainty has to be expected for the J value. On the other hand, while our calculations used a mean isotropic g value, it is likely that the theoretical curves depend on the g_{Cu}/g_{Mn} ratio[17,22] and on anisotropic factors.

The relatively low g value can be explained by such an uncertainty on the theoretical results, even if a g-value significantly lower than 2.0 can be expected in a compound containing coupled copper-manganese pairs.[23–26] For lack of T infinite paramagnetic limit, the determination of g at 240 K gives 1.94.[27]

The J value can appear large for copper and manganese

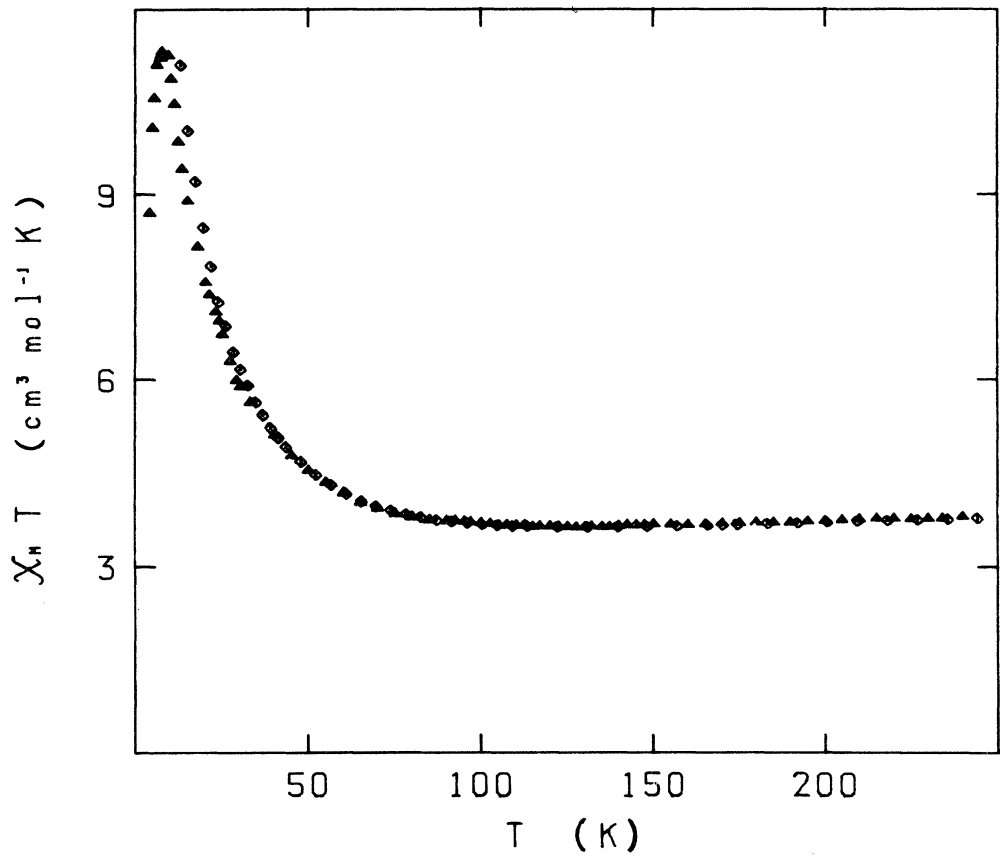

FIG. 7. Comparison of the experimental results of CuMnDTO (△) with the theoretical quantum-classical approach, for $J=-30.3$ cm^{-1} and $g=1.90$ (◇).

ions located at 6 Å from each other. But σ through-space exchange pathways are known to be very efficient in bridges similar to dithioxalato such as oxalato,[28,29] oxamido,[30–32] or dithioxamido.[33,34] We discuss the orbital mechanism of the interaction through the dithioxalato anion in Ref. 12.

B. One-dimensional character of CuMnDTO

The increase of $\chi_M T$ in a large temperature range (130–7.5 K) shows qualitatively that CuMnDTO is a rather good 1D chain ($|J'|$ interchain $\ll |J|$ intrachain).

Two ways are possible to appraise quantitatively the dimensionality in CuMnDTO.

(i) By determining the ratio of interchain-intrachain energies

$$\rho=J'S^2/JsS \ . \tag{35}$$

We determined the J' interchain coupling constant between manganese ions in PdMnDTO. If we expect that J' in CuMnDTO is the same, or close to, the one in PdMnDTO, we can derive $\rho=2.6\times10^{-2}$.[35]

(ii) By determining the correlation length in the temperature range where the ferrimagnetic short-range order is operating, and by neglecting, in first approximation, the copper(II) contribution to the susceptibility, we can estimate the number $n(T)$ of ferromagnetically coupled manganese spins, from the value of the susceptibility per spin χ_0, using the relation (6) in Ref. 10:

$$\chi_0=n(T)\beta g^2\mu_B^2 S(S+1)/3 \ . \tag{36}$$

At 7.9 K, $n\simeq10$, i.e., an estimate of 20 copper(II) and manganese(II) correlated spins. (In TMMC, one of the best 1D materials, $J'/J\simeq10^{-4}$ and $n\simeq3\times10^2$, just above the Néel temperature.) However, a 3D influence on the susceptibility seems already detectable at higher temperatures as can be seen in Fig. 8 and below.

C. Susceptibility divergence at low temperature

As the 1D character of CuMnDTO seems significant, it is of interest to study if the low-temperature behavior of the ferrimagnetic chain can be tested with the preceding theoretical calculations for 1D ferromagnets as far the divergence of χ_M at low temperature is concerned:

$$\chi_M=aT^{-\alpha} \ . \tag{37}$$

Our experimental susceptibility results are shown in Fig. 8(a) as plots of $\log\chi_M$ vs $\log T$. The slope α of the curve first increases in absolute value, seems constant, with $\alpha=1.57$, from 55–9 K and then decreases, when the 1D→3D crossover influence becomes evident. A great care is needed for the interpretation of the linear part of

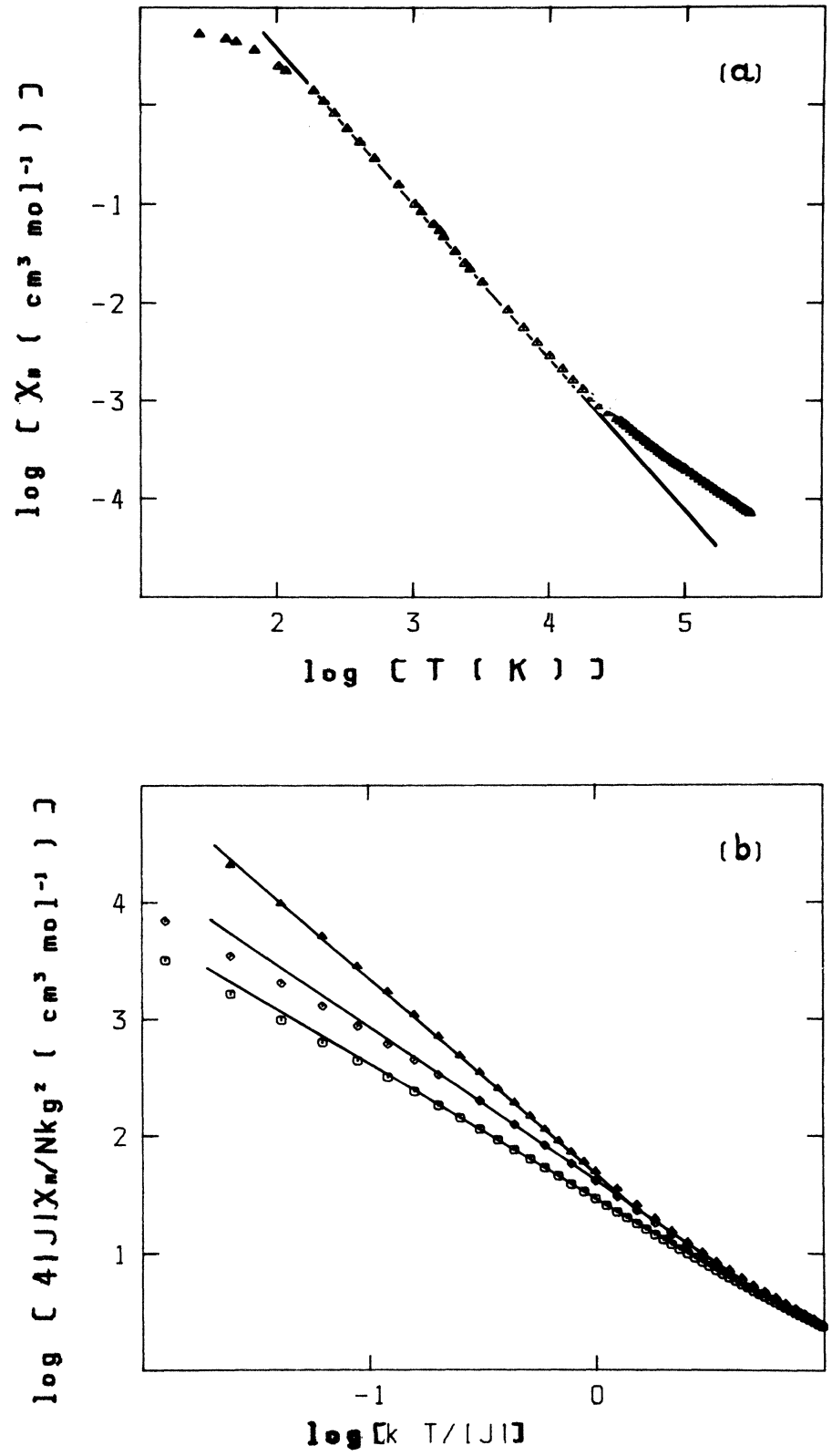

FIG. 8. (a) Experimental low-temperature behavior of the susceptibility of CuMnDTO as a plot of Napierian $\ln\chi_M$ vs $\ln T$. The straight line is a guide for the eye, corresponding to a slope $|\alpha| \simeq 1.57$. (b) Theoretical low-temperature behavior of χ_M as a plot of Napierian $\ln(\chi_M 4|J|/Nkg^2)$ vs $\ln(kT/|J|)$. Curve 1: quantum ring with $N=2$(□); curve 2: quantum ring with $N=3$(◇); curve 3: quantum-classical chain (△). The straight lines drawn are guides for the eye, corresponding to slopes $|\alpha| \simeq 1.15$, 1.33, and 1.69, respectively.

the curve: It can correspond to the low-temperature behavior of the ferrimagnetic chain and in this case $\alpha=1.57$ has to be compared with the preceding calculated values for 1D F chains, by Fisher[36] from the Heisenberg model of infinite spin ($\alpha=2$), by Bonner and Fisher[21] from a quantum $\frac{1}{2}$ spins chain ($\alpha=1.8$), by Baker *et al.*[37] with the expansion method ($\alpha=1.67$), or by Blöte on quantum $\frac{1}{2}$ spins chain ($\alpha=1.5$);[38] it can correspond also to a compromise between the 1D ferrimagnetic behavior, and the 3D influence becoming operative around 27 K [see Fig. 8(a)]. We report in Fig. 8(b), the theoretical results described in Sec. V. The maximum slope obtained in the linear part of the curve obtained with the quantum-classical model is $\alpha=1.69$.[39]

The values obtained with the quantum-rings approach, shown in Fig. 8(b) are of less interest: The maximum slope α is 1.33 for the $N=3$ copper-manganese-pairs case since the low-temperature range is dominated by the $S=2N$ [Eq. (6)] spin state of the ring as $kT/|J|$ tends to zero.

D. Conclusion

The quasi-one-dimensional compounds CuMn $(S_2C_2O_2)_2\cdot 7.5H_2O$, CuMnDTO was synthesized, its crystal structure refined, and its one-dimensional ferrimagnetic behavior characterized, both experimentally (by susceptibility and magnetization measurements), and theoretically. A J/κ intrachain value equal to -43.6 K (-30.3 cm^{-1}) was determined. Synthetic endeavors on similar systems and studies of dynamic properties are currently underway.

ACKNOWLEDGMENTS

We wish to thank Professor O. Kahn and Dr. P. Veillet for helpful discussions and Dr. E. Velu for experimental help.

[1]See, e.g., *Magnetic Chains in Physics in One-dimension,* edited by J. Bernasconi and T. Schneider (Springer, Berlin, 1981), Part III.

[2]See, e.g., in *Extended Linear Chain Materials,* edited by J. S. Miller (Plenum, New York, 1983).

[3]See, e.g., R. D. Willett, J. C. Bonner, and L. J. de Jongh, in *Magneto-structural Correlations in Exchange-coupled Systems,* edited by D. Gatteschi, O. Kahn, and R. D. Willett, NATO Advanced Study Institute Series, (Reidel, Dordrecht, in press).

[4]C. Dupas, and J. P. Renard, Phys. Rev. B 18, 401 (1978).

[5]C. P. Landee and R. D. Willett, Phys. Rev. Lett. 43, 463 (1979).

[6]C. Dupas and J. P. Renard, in *Proceedings of the 1980 Annual Conference of the Condensed Matter Division of the European Physical Society, Antwerpen, Belgique, 1980,* edited by J. T. Devreese *et al.* (Plenum, New York, 1981).

[7]W. E. Hatfield, J. Appl. Phys. 52, 1985 (1981).

[8]J. C. Bonner and H. W. J. Blöte, Phys. Rev. B 25, 6959 (1981).

[9]J. C. Bonner, S. A. Friedberg, H. Kobayashi, D. L. Meier, and H. W. J. Blöte, Phys. Rev. B 27, 248 (1983).

[10]C. Dupas, J. P. Renard, J. Seiden, and A. Cheikh-Rouhou, Phys. Rev. B 25, 3261 (1982).

[11]A. Gleizes and M. Verdaguer, J. Am. Chem. Soc. 103, 7373 (1981).

[12]A. Gleizes and M. Verdaguer, J. Am. Chem. Soc. (to be published).

[13]H. W. J. Blöte, J. Appl. Phys. 50, 7401 (1979).

[14]M. Verdaguer, M. Julve, A. Michalowicz, and O. Kahn, Inorg. Chem. 22, 2624 (1983).

[15]E. Velu, R. Megy, and J. Seiden, Phys. Rev. B 25, 4429 (1983).

[16]J. A. Puertolas, R. Navarro, F. Palacio, D. Gonzales, R. L. Carlin, and A. J. van Duyneveldt, J. Mag. Mag. Mater. 31-34, 1067 (1983).

[17]J. Seiden, J. Phys. (Paris) Lett. 44, L947 (1983).

[18]Such an argument would be entirely convincing if the calculations had been derived in a well-defined physical model: For instance, an alternating chain of s quantum spins and S classical spins, if rigorously treated, doubtless would present no phase transition at finite temperature. As, in our treatment, the spins S are considered as classical before (13) and then treated as quantum operators, the argument is weaker.

[19]Our numerical calculations were performed at the Centre Inter-Regional de Calcul Electronique de Centre National de la Recherche Scientifique, Orsay, using an Amdahl 470/V7 computer. The home-written program used double-precision EISPACK matrix diagonalization programs TRED2 and TQL2. [M. Verdaguer, thesis, Université de Paris—Sud Orsay, 1984 (unpublished)].

[20]R. Orbach, Phys. Rev. 115, 1181 (1959).

[21]J. C. Bonner and M. E. Fisher, Phys. Rev. 135, A640 (1964).

[22]M. Drillon, J. C. Gianduggo, and R. Georges, Phys. Lett. 96A, 413 (1983).

[23]E. Buluggiu, A. Vera Z. Naturforsch. 31a, 911 (1976).

[24]E. Buluggiu, J. Phys. Chem. Solids 41, 1175 (1980).

[25]J. A. Paulson D. A. Krost, G. L. McPherson, R. D. Rogers, and J. L. Atwood, Inorg. Chem. 19, 2519 (1980).

[26]L. Banci, A. Bencini, and D. Gatteschi, Inorg. Chem. 20, 2734 (1980).

[27]This g value gives of course a less good fit than the one shown in Fig. 7. To rule out uncertainties due to the determination of g and J on one point, we fitted the theoretical curve in Fig. 7 by an empirical expression. The least-squares fit of our experimental results with this expression, in the temperature range 20—240 K gave results quite similar to the first one: $J=-28.3$ cm^{-1} and $g=1.904$. For details, see Ref. 12.

[28]J. J. Girerd, O. Kahn, and M. Verdaguer, Inorg. Chem. 19, 274 (1980).

[29]M. Julve, M. Verdaguer, O. Kahn, A. Gleizes, and M. Philoche-Levisalles, Inorg. Chem. 22, 368 (1983).

[30]M. Nonoyama and K. Nonoyama, J. Inorg. Nucl. Chem. 43, 2567 (1981).

[31]T. R. Felthouse, Ph. D. thesis, University of Illinois, 1978 (unpublished), cited by D. N. Hendrickson in Ref. 3.

[32]M. Julve, M. Verdaguer, and O. Kahn (unpublished results).

[33]J. J. Girerd, S. Jeannin, Y. Jeannin, and O. Kahn, Inorg. Chem. 17, 3034 (1978).

[34]C. Chauvel, J. J. Girerd, Y. Jeannin, O. Kahn, and G. Lavigne, Inorg. Chem. 18, 3015 (1979).

[35]Such an assumption is likely: The CuS_4 groups stack in a staggered configuration, with δ overlap between dxy orbitals,

a copper-copper distance of 3.68 Å, and a sulfur-sulfur distance $\simeq$3.9 Å greater than the van der Waals one (see Fig. 2), which seems sufficient to hinder a significant interaction. Nevertheless, we try to verify this point by synthesizing a copper bimetallic chain with a diamagnetic ion instead of manganese.

[36]M. Fisher, Am. J. Phys. 32, 343 (1964).

[37]G. A. Baker, G. S. Rushbrooke, and H. E. Gilbert, Phys. Rev. 135, A1272 (1964).

[38]J. C. Bonner, private communication about recent calculations by H. W. J. Blöte.

[39]At low values of $kT/|J|$ (i.e., <0.2) and very large values of matrix elements, we observed numerical instability and results that are not reported.